TOHOKU UNIVERSITY IRIDeS
International Research Institute of Disaster Science

NIPPON KOEI

A digital twin system for urban-scale earthquake damage assessment integrating simulation and sensor network

Sponsored by

TOKIO MARINE GROUP

Contents

Executive Summary

A Digital Twin System for Urban-scale Earthquake Damage Assessment

As one of the world's most earthquake-prone nations, Japan has experienced diverse forms of damage from past earthquakes. To mitigate damage and achieve rapid recovery, it is necessary to obtain a comprehensive city-scale assessment of building damage immediately after an earthquake.

In this study, we propose a framework that integrates simulation with seismic sensor network to enable real-time prediction of building damage across entire cities during an earthquake. Figure 1 illustrates the concept of this framework. In this framework, earthquake simulations for the entire target city are conducted in advance, before an actual earthquake occurs. The simulations numerically model how seismic waves generated at the fault propagate through the subsurface and are subsequently transmitted to buildings, inducing dynamic responses.

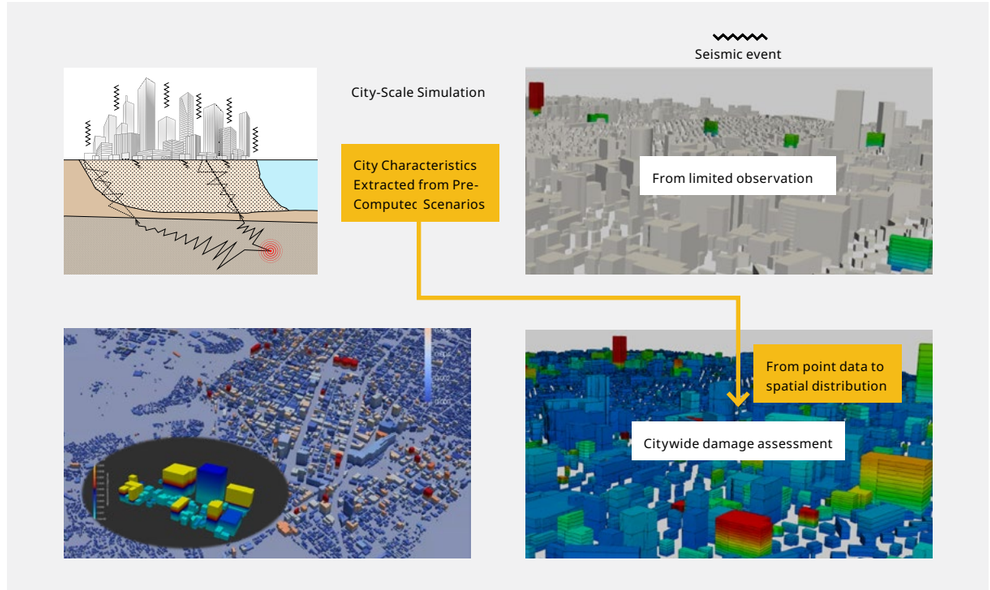

Figure 1 Conceptual framework for earthquake damage assessment.

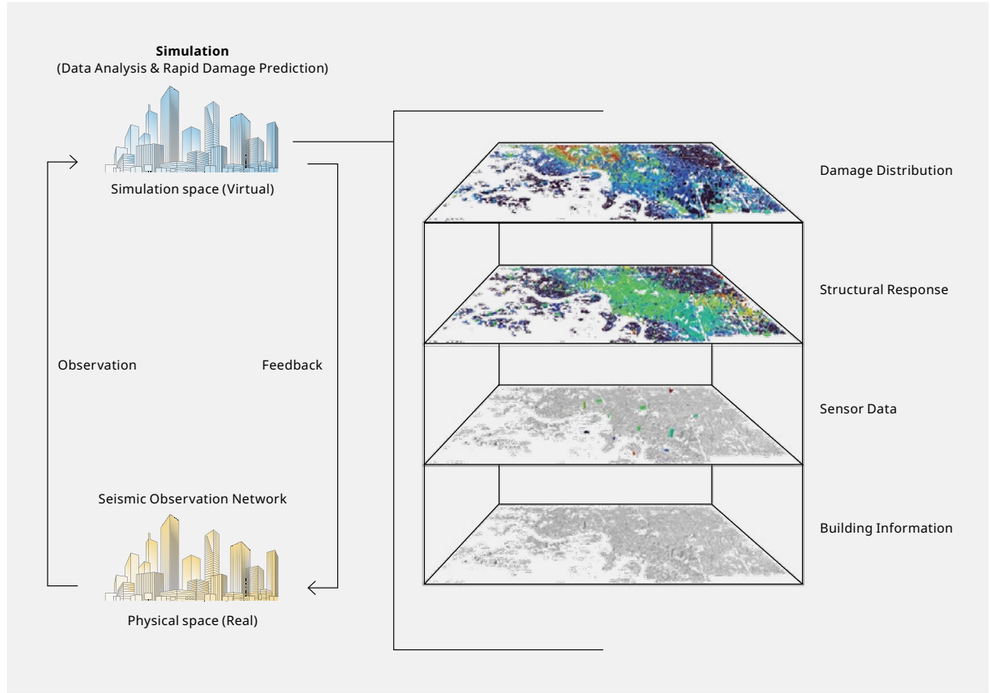

Figure 2 Conceptual diagram of the digital twin system "SAMRRAi".

The results are then interpreted as the level of damage. By comprehensively analyzing these results, the spatial characteristics of building damage within the city can be identified beforehand. When an actual earthquake occurs, these pre-identified spatial characteristics are combined with vibration data from specific buildings obtained through the existing sensor network. The proposed framework then enables real-time evaluation of earthquake damage across the entire city.

To demonstrate the performance of proposed framework, we have developed a “digital twin system” as the prototype of this technology and named as SAMRRAi (Seismic Assessment and Monitoring system for Real-time Risk Analysis). As shown in Figure 2, a “digital twin” reproduces the real world within a simulation (virtual or digital) space, creating an environment that closely mirrors reality based on information obtained from the physical world. This enables the exchange of information between the real and simulation spaces as a twin. In this study, various types of data obtained from physical space such as building information, ground conditions, and fault models along with real-time sensor data from the seismometer network, are integrated to analyze within the simulation space. Consequently, the digital system can provide real-time information on damage assessment to the physical (real) world.

To verify the effectiveness of the proposed earthquake damage assessment framework and the SAMRRAi system, the developed framework is applied to a part of Sendai City, Miyagi Prefecture, assuming an inland earthquake caused by fault movement along the Nagamachi–Rifu fault zone. Figure 3 shows an example of the visualization of the simulation results. In addition, various risk indicators can be calculated from the simulation results using various functions for not only the overall structural damage but also the damage to various internal components of buildings, such as ceilings, interior walls, piping, furniture, and sprinklers.

Figure 4 shows the system interface of SAMRRAi, which displays seismic data collected from sensors installed at specific locations throughout the city (see red label). At the initial stage, information is limited to buildings where sensors are installed. However, by applying the proposed SAMRRAi framework, the real-time data from the sensor network are integrated with pre-simulated seismic response data and spatial damage characteristics. This integration enables a rapid and comprehensive estimation of damage to all buildings across the city, including those without installed sensors.

As a result, Figure 5 presents rapid estimations obtained once the sensor network detects seismic data during an earthquake. It shows the spatial distribution of the predicted damage levels for all buildings in the city as one of the optional risk assessment indicators. This visualization provides valuable insights into the overall impact of the earthquake and supports decision-making for emergency response, resource allocation, and future risk mitigation planning.

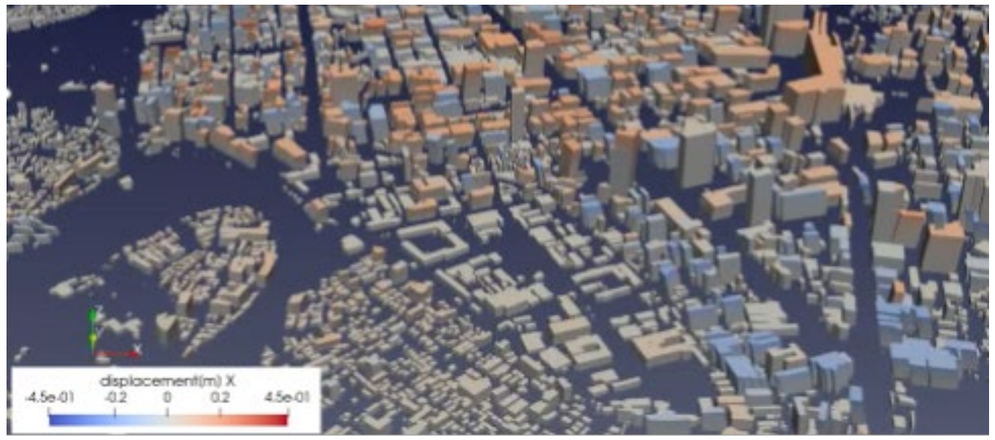

Figure 3 Example of simulation results.

Figure 4 Sensor data at observation points.

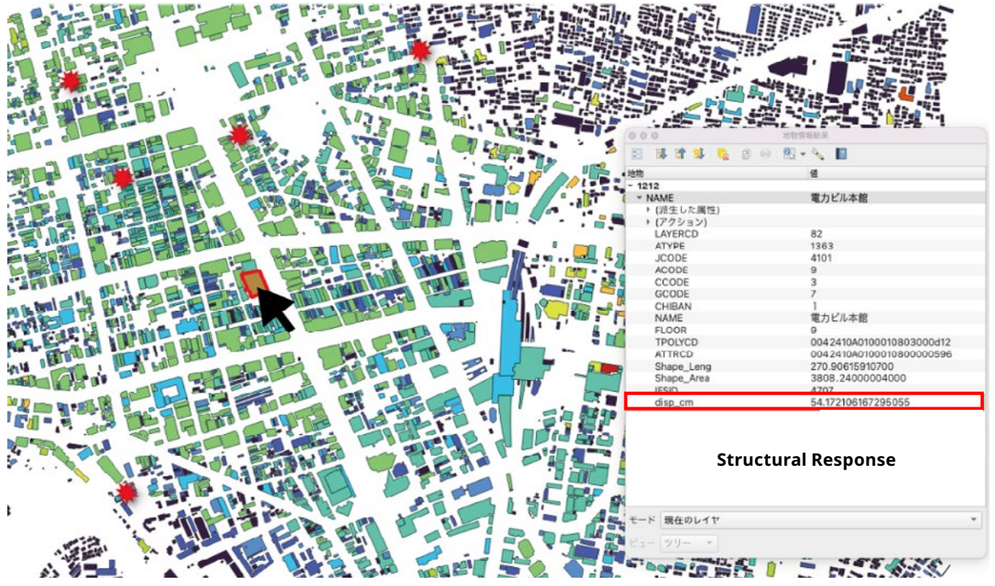

Figure 5 Risk assessment indicators for buildings not equipped with observation points.

1.0
Background, Purpose, and Summary of Research Findings

This research is part of the achievements of the Nippon Koei Resilient City Technology Joint Research Division at the International Research Institute of Disaster Science, Tohoku University. The division, established in April 2022, is a collaboration between Tohoku University and Nippon Koei Co., Ltd. Its mission is to advance the construction of resilient cities through the application of various technologies in data science. The core research effort is the development of digital twin models for high-speed, high-precision disaster prevention and mitigation, utilizing data-driven approaches and large-scale simulations to enable real-time integration between the digital and real worlds.

Figure 1 Kumamoto earthquake in 2016.

Figure 2 Noto Peninsula earthquake in 2024.

1.1 Research Background

As one of the world's most earthquake-prone nations, Japan has experienced diverse forms of damage from past earthquakes. In recent years, inland earthquakes directly beneath the surface, particularly those with seismic intensity 7, such as the 2016 Kumamoto Earthquake, the 2018 Hokkaido Eastern Iburi Earthquake, and the 2024 Noto Peninsula Earthquake, have caused extensive damage to buildings and social infrastructure near fault lines (Figures 1 and 2).

This has also resulted in cascading impacts, including blackouts, damage to lifelines, prolonged evacuation periods, and decreased economic activity. To mitigate earthquake damage and enable rapid recovery, it is essential to receive urban-scale damage assessments as soon as possible after an event, providing an overview of the entire affected area.

In recent years, advances in simulation technology and computing power have made it possible to evaluate the impact of earthquakes on entire urban areas at once. However, simulations require the consideration of various complex input data, including seismic characteristics, ground conditions, and structural information. Consequently, achieving high-fidelity results often demands a significant computational time. Therefore, if we follow the conventional framework to gather data and start earthquake simulations only after an actual event, we cannot provide the necessary information needed for disaster response in a short period.

In parallel, seismic sensor technology has become more sophisticated, leading to a gradual increase in installations on private buildings alongside public infrastructure. This expanding network is valuable because the measured seismic motion provides data for estimating localized building damage during an earthquake. However, the number of seismometers is still insufficient, limiting our ability to accurately assess the overall damage situation across an entire city in real time.

Urban-scale earthquake simulations and seismic sensor technologies described thus far have primarily developed independently within their respective fields. A gap remains between the digital (simulation) and actual worlds. Therefore, this research proposes a new framework for earthquake damage assessment by effectively integrating simulations and seismic sensor network. Furthermore, a platform based on the proposed framework has been developed. Details of the development are provided in the following section.

1.2 The proposed framework for real-time earthquake damage assessment

We propose a framework that integrates simulation and seismic sensor networks to enable the real-time prediction of building damage across an entire city during an earthquake. This concept is illustrated in Figure 3. The framework involves conducting comprehensive earthquake simulations for the entire target city in advance. These simulations model the propagation of seismic waves from the fault, through the soil layers, and finally to the ground surface. The results are then used as input to compute the dynamic response of buildings and identify potential damage across the city. By running these simulations with comprehensive cases and analyzing the results, the spatial characteristics of building damage in the city are pre-determined. When an actual earthquake occurs, this pre-determined spatial damage profile is combined with real-time seismic wave input data from the existing sparse sensor network. This integration enables a rapid, real-time assessment of earthquake damage across the entire city.

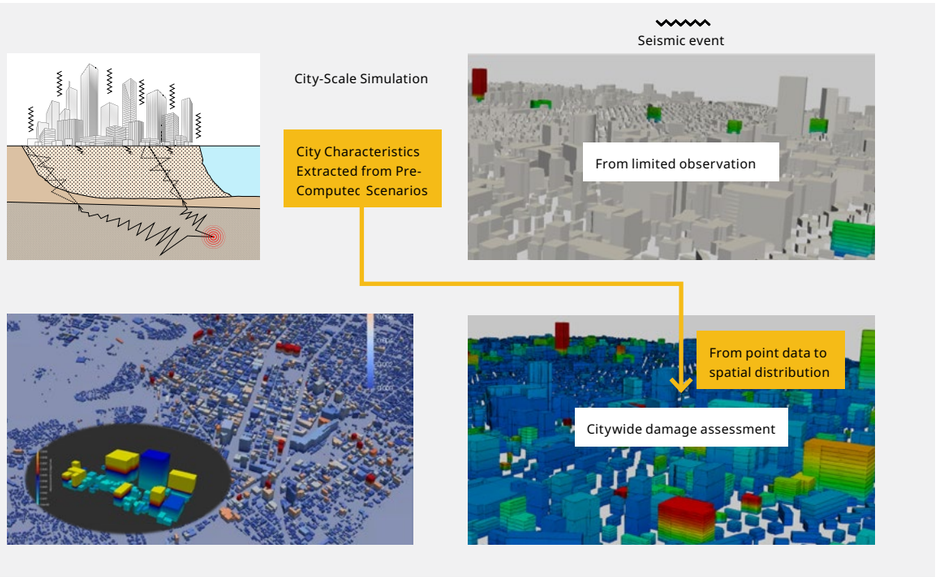

Figure 3 Concept of real-time earthquake damage assessment.

1.3 Development of Platform for the Digital Twin System

We developed a digital twin system as a platform for earthquake risk assessment, implementing the generation of simulation input data, visualization of results, and the framework for real-time earthquake damage assessment.

This system is named SAMRRAi (Seismic Assessment and Monitoring system for Real-time Risk Analysis). Figure 4 shows its conceptual diagram.

A “digital twin” refers to a technology that reproduces a counterpart of the physical world (the twin) within a virtual space (digital model or simulation) based on real-world data. This enables continuous exchange of information between physical and virtual spaces according to specific objectives.

In this research, we are developing a digital twin system that integrates various real-world data (e.g., buildings, ground conditions, active faults) from real-time sensor networks with large-scale earthquake simulations, thereby enabling real-time feedback on building damage to the physical world.

In this study, to confirm the performance of the proposed framework for real-time earthquake damage assessment, we verified it by applying the framework to an actual city under earthquake scenarios with potential occurrence. Specifically, we constructed a prototype of SAMRRAi for Sendai City, Japan. Subsequent chapters describe the methodologies and details of the risk assessment techniques, along with the verification results and the SAMRRAi prototype.

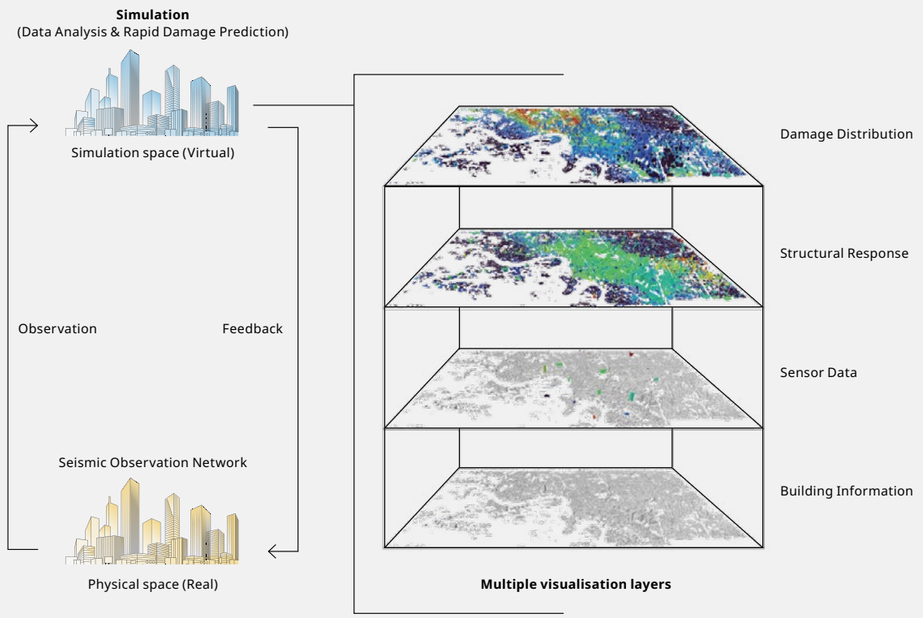

Figure 4 Conceptual diagram of the SAMRRAi digital twin system..

2.0
Case Study for Verification, Simulation Method, and Risk Assessment Indicator

Here, we describe the target city and the earthquake scenarios, the simulation method required for evaluation, and the risk assessment indicator.

2.1 Target City, Seismic Fault, and Earthquake Scenarios

The synthetic earthquake considered in this study is an inland event occurring directly beneath the city, associated with fault movement along the Nagamachi–Rifu fault zone. The study area covers a portion of Aoba Ward, Sendai City, Miyagi Prefecture (Fig. 5). The Nagamachi–Rifu fault zone is an active fault located along the western edge of the Sendai Plain. The probability of an earthquake occurring along this fault within the next 30 years is considered moderately high, with an expected maximum intensity of about seismic intensity 7. Furthermore, since Sendai City is located near the fault, the earthquake is expected to cause serious damage.

As mentioned earlier, the proposed framework requires conducting multiple simulations in advance, taking into account different earthquake scenarios (analysis cases with varying conditions).

In this study, based on information on the source faults of the Nagamachi–Rifu fault zone published by J-SHIS [1], we created 13 scenarios with magnitudes (Mw) ranging from 6.3 to 7.5. Figure 6 shows the locations of the fault and asperities as provided by J-SHIS. An asperity refers to a locked region on the fault plane that experiences particularly large slip during fault rupture. In the source fault model used here, two asperities are included: the first asperity (red box) and the second asperity (blue box). The star symbol in the figure indicates the hypocenter, which is the initiation point of rupture along the fault. When varying the magnitude, it is also necessary to account for changes in asperity size and location, as well as the position of the hypocenter. Taking these factors into account, we constructed the 13 earthquake scenarios described above.

Figure 5 Target area (part of Aoba ward, Sendai city; 32,334 buildings).

2.2 Simulation Method

In this section, we describe the specific procedures and methods used to simulate building damage caused by earthquakes. As shown in Figure 7, seismic motion originates at the fault and propagates through the engineering bedrock (relatively stiff layers with S-wave velocities of 300–700 m/s) and the surface soil layers (relatively soft layers), where it may be amplified or attenuated. The seismic motion then reaches buildings, causing structural damage.

This entire process needs to be represented in the simulation. However, it is difficult to capture all stages continuously using a single method.

Therefore, we conduct the three processes separately: propagation through the engineering bedrock, propagation through the surface soil (site response), and building response.

The same simulation process is performed for all 13 earthquake scenarios described earlier, evaluating the seismic response of all buildings within the study area. In the following sections, we provide a detailed description of each of these three simulation processes.

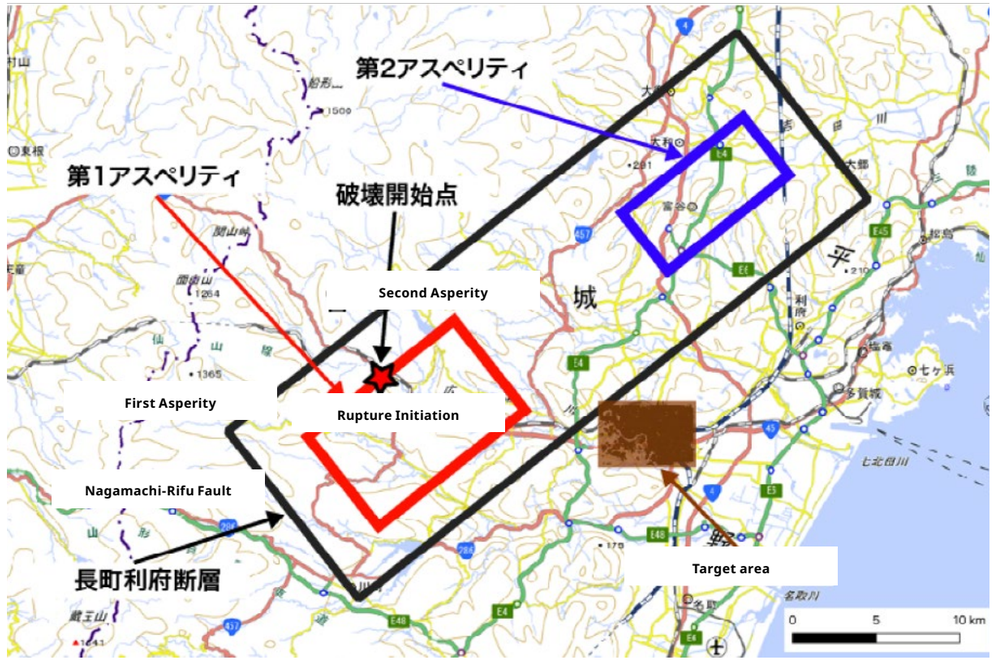

Figure 6 Source fault model for the Nagamachi-Rifu fault zone [1].

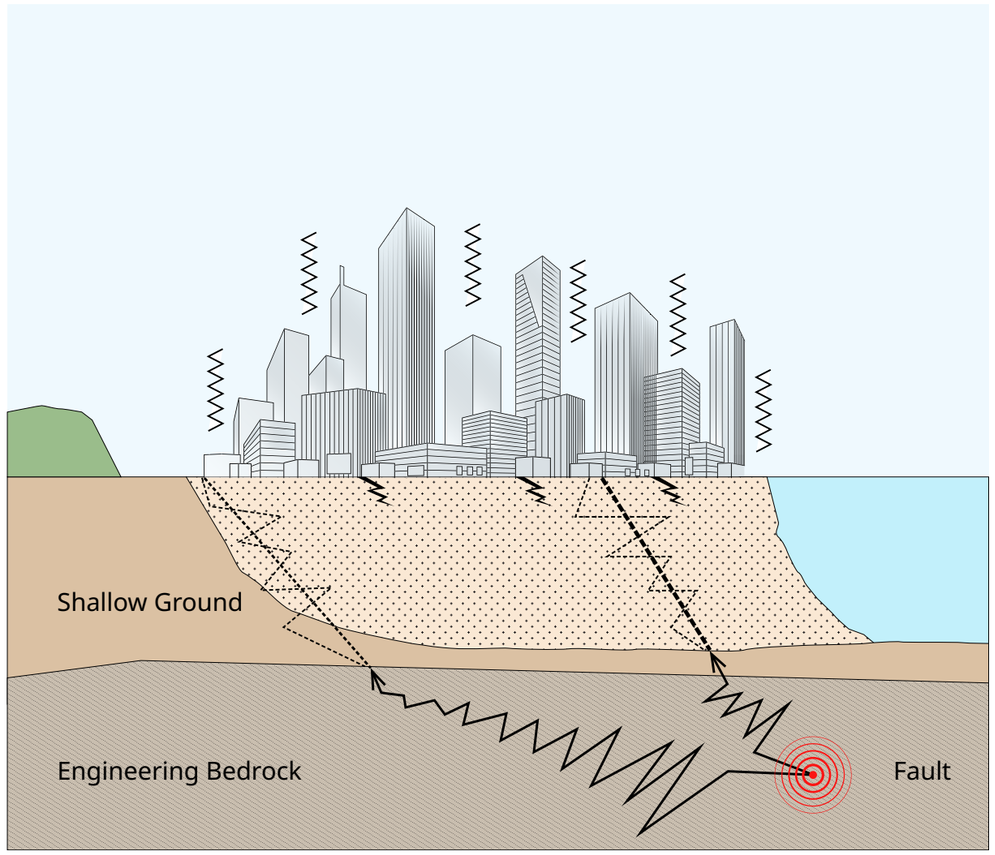

Figure 7 Conceptual diagram of seismic wave propagation and building response.

2.2.1 Propagation Analysis in the Engineering Bedrock

Among the three processes described above, this section explains the simulation of seismic wave propagation from fault rupture through the engineering bedrock up to the engineering bedrock surface (the boundary between the engineering bedrock and the surface layers). Methods capable of performing this calculation can be broadly classified into theoretical, semi-empirical, and hybrid approaches. Since past earthquake records for the target Nagamachi–Rifu fault zone are insufficient, we employed a semi-empirical method, namely the stochastic Green's function method [2,3].

The stochastic Green's function method generates seismic waveforms using a statistical approach, synthesizing them as Green's functions.

A key feature of this method is that it allows the generation of seismic waveforms even at sites where sensor records are sparse or unavailable. In practice, the target fault plane is divided into a grid of subfaults, and for each subfault, the element earthquake's time-dependent and phase characteristics are incorporated to generate its Green's function (time-history waveform). By summing up the Green's functions of all subfaults, seismic waves at any point on the engineering bedrock surface can be obtained.

In this study, we used the stochastic Green's function program published by J-SHIS [4] to evaluate the seismic wave at points on the engineering bedrock surface corresponding to the location of each building.

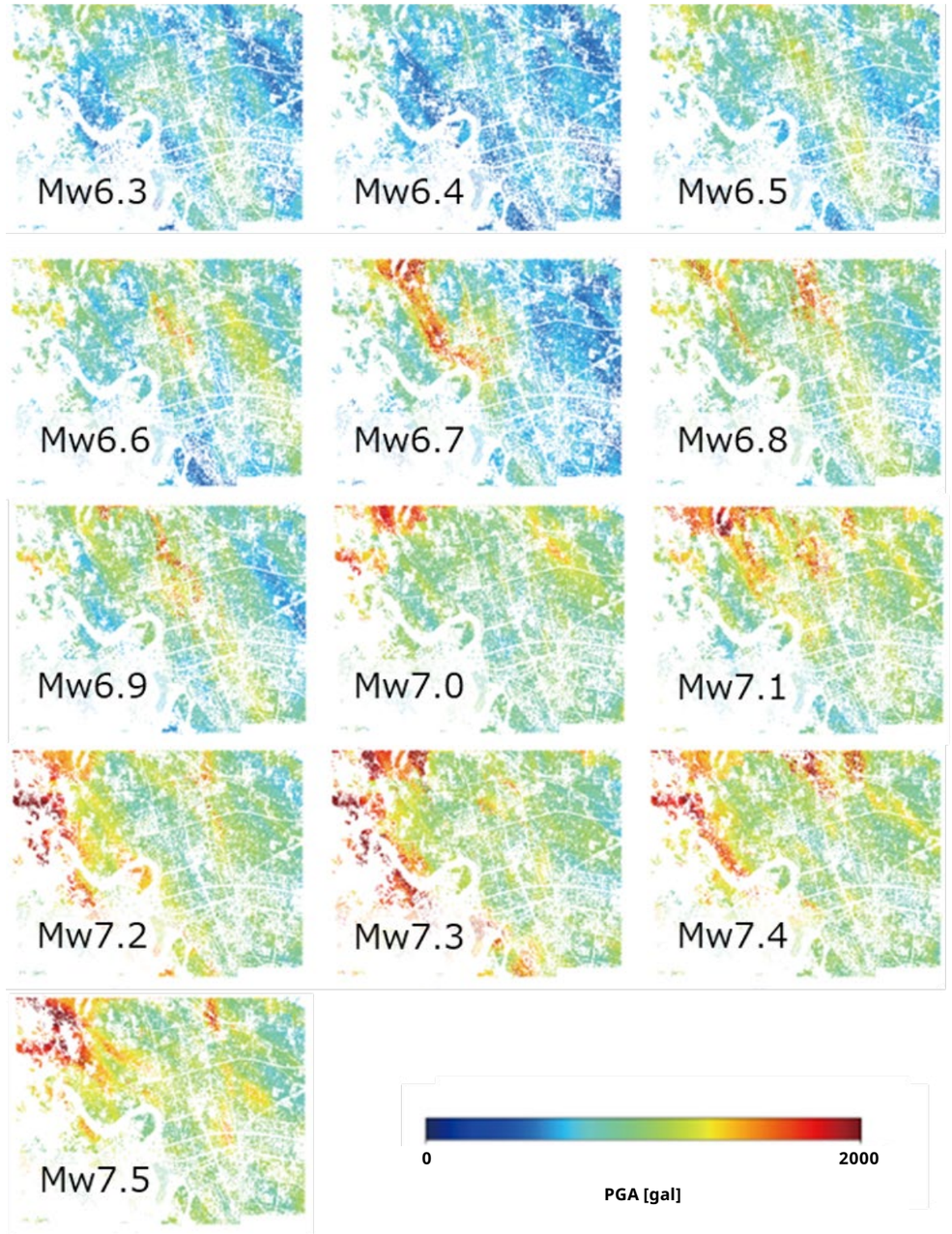

Figure 8 Maximum ground acceleration (PGA) distribution at the ground surface for each scenario obtained from site response analysis.

2.2.2 Site Response Analysis

Next, we describe site response analysis, which accounts for the amplification or attenuation of seismic waves as it propagates through the surface layers. For this simulation, we used the site response analysis module of the Integrated Earthquake Simulation (IES) system [5]. The IES site response analysis adopts an equivalent linear analysis, which allows the propagation of seismic waveforms from the engineering bedrock directly beneath each building up to the ground surface to be simulated. Equivalent linear analysis is a simplified approach to modeling the complex behavior of the ground. As described above, seismic waves at the engineering bedrock beneath each building are generated using the stochastic Green's function method.

These waveforms serve as input for the propagation and amplification analysis through the surface soil layers, generating seismic waveforms at the ground surface corresponding to each building's location. The site response analysis is conducted for all buildings in the study area for each earthquake scenario. Figure 8 illustrates the surface distribution of peak ground acceleration (PGA) obtained from the site response analysis for the various scenarios. Although these figures present the maximum acceleration values as snapshots, the actual simulation results provide time-history data for every building location.

2.2.3 Building Response Analysis

Then, the building response analysis is performed using the ground surface waveforms from the site response analysis. In this step, we adopted a Multi-Degree-of-Freedom (MDOF) model, a type of building response analysis implemented in the IES system. As shown in Figure 9, the MDOF model represents a building as a series of masses and springs. The number of point masses is defined to correspond to the number of floors, with their magnitudes corresponding to the mass of each floor. The stiffness of each spring is then estimated based on building type, as well as the number and magnitude of the point masses. The stiffness of each spring is estimated based on the building type, number of masses, and mass of each mass. The building types considered are reinforced concrete (RC), wooden, and steel structures, and the data for each building is prepared according to its specific characteristics. Figure 10 visualizes the building response at a certain time for a scenario with Mw 6.9.

The color of each building in the figure represents the magnitude of displacement induced by the seismic motion. While the buildings appear to have complex shapes in the visualization, this is purely for illustrative purposes; the actual analysis is based on the MDOF model described earlier. Figure 11 shows the distribution of representative response displacements obtained from the building response analysis results for each scenario. Indicators used to estimate building damage include representative response displacement, maximum acceleration, inter-story drift angle, and spectral intensity (SI) values, all of which can be determined from the simulation results. Here, representative response displacement is used as an example. This indicator is closely related to building damage levels calculated using the Capacity Spectrum Method (CSM), which is described in detail later. From these figures, it can be observed that larger earthquake magnitudes lead to higher building damage levels, and that the distribution of damage exhibits characteristics specific to the study area.

Figure 9 A Multi-Degree-of-Freedom (MDOF) model.

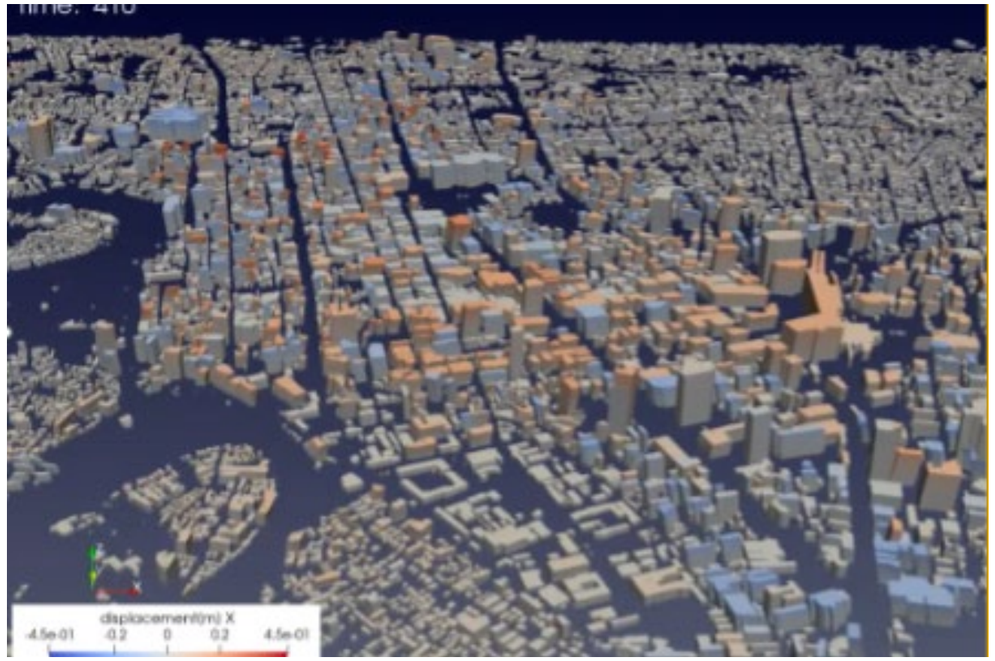

Figure 10 Snapshot visualizing the results of the building response analysis.

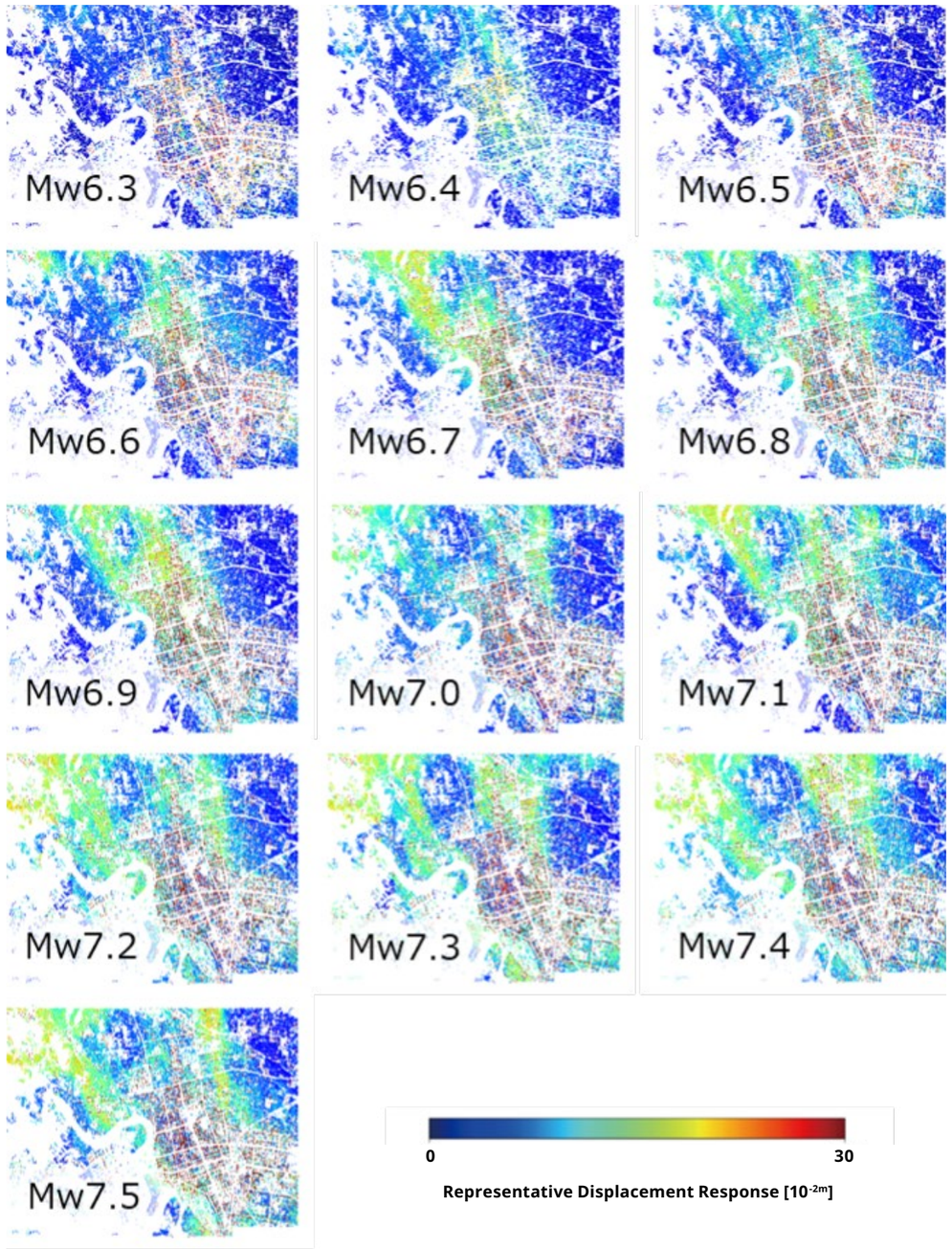

Figure 11 Distribution of representative response displacements for each scenario evaluated using CSM.

2.3 Earthquake Risk Evaluation Indicators

So far, we have described the simulation methods. Here, we explain the risk evaluation indicators used in this study. Since the simulation results provide time-history data of all buildings' responses for all scenarios, a variety of risk indicators can be established. Earthquake risk is a quantitative measure of the potential damage or loss caused by an earthquake. It is evaluated by relating risk indicators representing building damage or loss to either ground motion intensity measures or structural response values.

Focusing on ground motion intensity measures, common indicators include seismic intensity, Peak Ground Acceleration (PGA), Peak Ground Velocity (PGV), response spectra, and spectral intensity (SI) values. While seismic intensity and peak ground motion are convenient to use, they do not fully reflect the frequency characteristics of the ground motion. In contrast, response spectra and SI values account for the frequency characteristics of seismic motion and are generally considered to correlate well with building damage. However, the most appropriate indicator can vary depending on the type of structure, the non-structural components, and the level of damage. Therefore, estimating damage using a single indicator alone is difficult. Table 1 summarizes structural response values that are generally regarded as factors contributing to damage in various building components.

Component	**Item**	**Main Indicators** (Structural Response Values)
Structure		Maximum inter-story drift angle, Maximum response acceleration
Building Non-Structural Components (Acceleration dependent)	Roofs, ceilings, furniture, fixtures, etc.	Maximum response acceleration
Building Non-Structural Components (Displacement dependent type)	Exterior walls, partition walls, non-load-bearing walls, etc.	Maximum inter-story drift angle
Building Equipment	Piping, sprinklers, elevators, etc.	Maximum response acceleration, Maximum response speed

There are two types of risk indicators representing building damage and loss: those based on thresholds and those based on fragility functions. Threshold-based risk assessment deterministically evaluates damage by setting thresholds at which each damage level, such as "total collapse" or "moderate damage," occurs for seismic intensity measures or structural response values, and comparing observed values with these thresholds.

On the other hand, risk assessment using fragility functions calculates the probability of each damage level occurring by categorizing buildings according to structural type and construction era. This allows probabilistic risk assessment based on past earthquake records and experiments. From this, indicators such as PML (Probable Maximum Loss), which evaluates physical loss amounts, and BI (Business Interruption), which evaluates building

downtime, can be defined, and the appropriate indicator is selected according to the evaluation purpose. For example, PML is used for planning restoration costs and calculating earthquake insurance payouts, while BI serves as a reference for determining business continuity. In the digital twin system developed in this study, it is assumed that both deterministic and probabilistic seismic risk assessments can be performed using various "seismic intensity measures" and "structural response values." In deterministic risk assessment, threshold values are set for maximum inter-story drift angle and maximum response acceleration for each component. In probabilistic risk assessment, fragility functions constructed in relation to the capacity spectrum method are used. This method is adopted in the damage estimation system HAZUS of the Federal Emergency Management Agency (FEMA, United States). By inputting representative structural response values obtained from CSM into fragility functions, it is possible to estimate the probability of damage for structural components, deformation-dependent non-structural components, and acceleration-dependent non-structural components. Because both structural and non-structural components can be evaluated from the same simulation results, this provides evidence for more in-depth discussion of disaster prevention and mitigation.

Fig. 12 shows an example of deterministic probabilistic seismic risk assessment for a Mw 6.9 scenario, presenting the damage to structures and non-structural components (both deformation-dependent and acceleration-dependent). In this figure, damage levels (i.e., none, slight, moderate, extensive, complete) are classified based on the calculated risk indicator values, and their proportions are shown in a pie chart. From this figure, it can be confirmed that the number of buildings classified as "slight" damage, shown in green, increases with magnitude. It can also be observed that non-structural components tend to sustain greater damage than structural components. Thus, even for the same earthquake, results differ depending on the evaluation target, making it a significant advantage to be able to assess risk using various indicators.

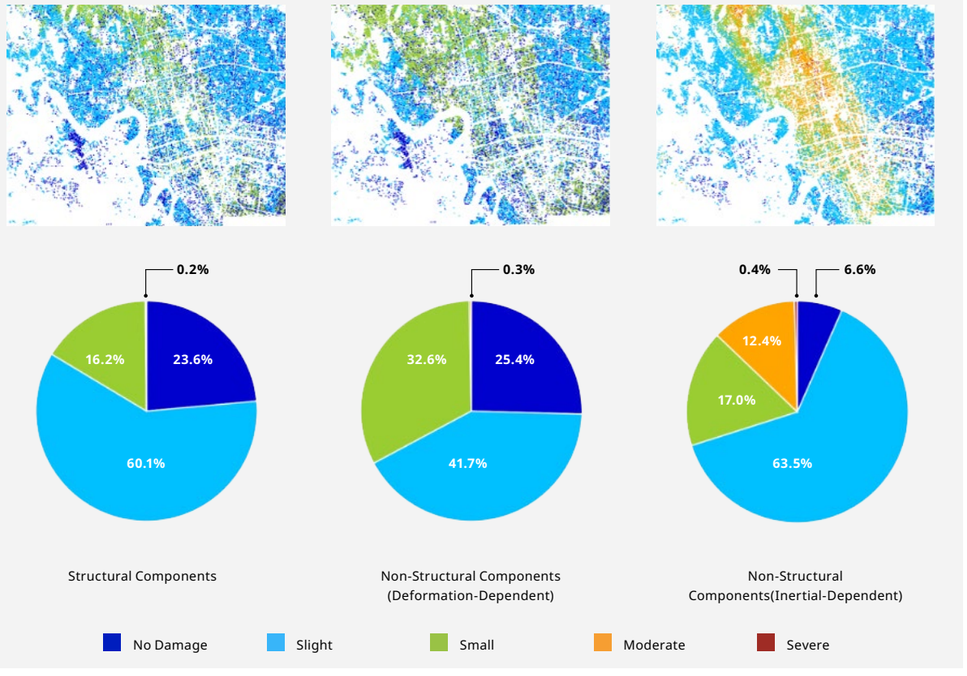

Figure 12 Comparison of damage to structural and non-structural components caused by earthquakes.

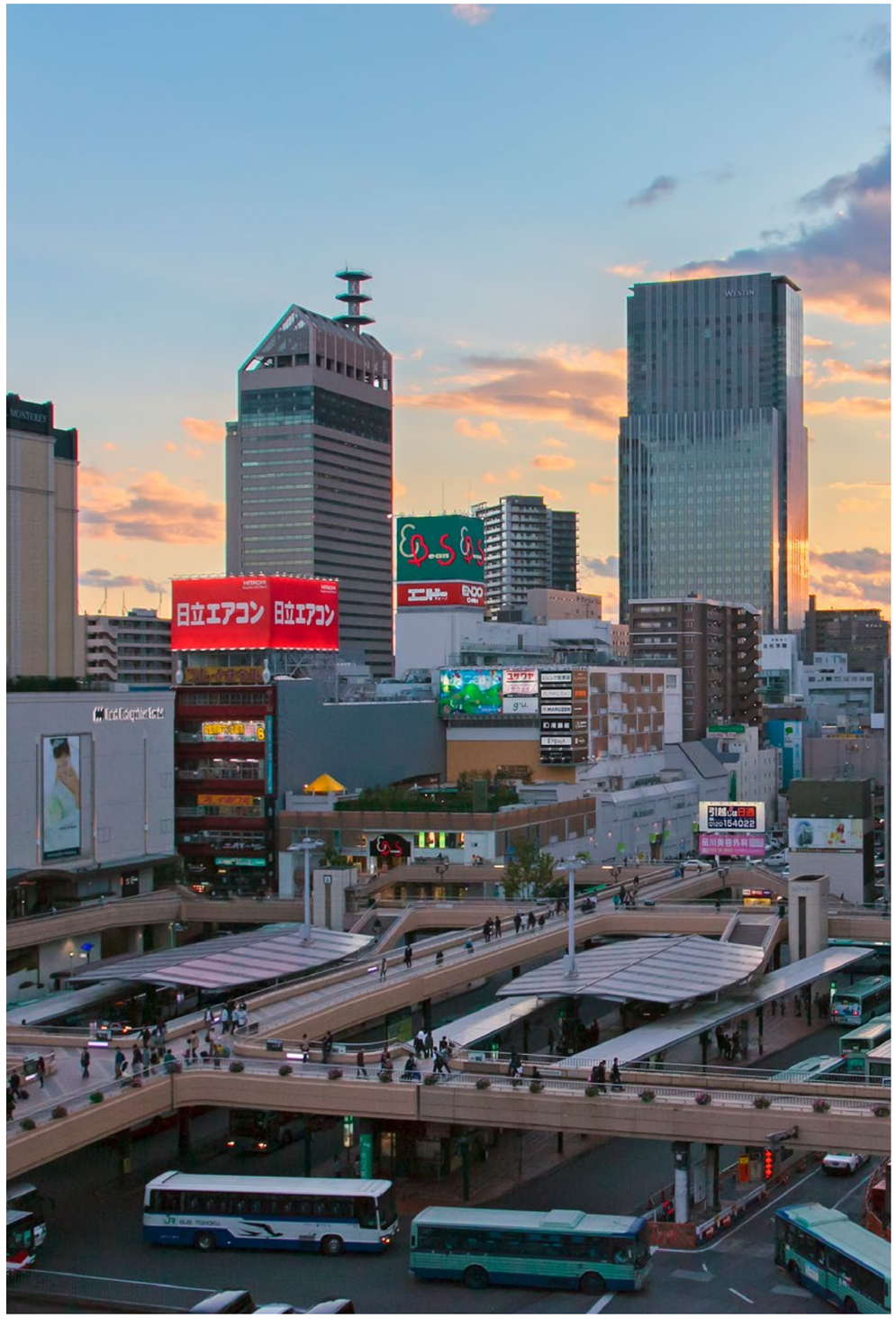

3.0
Real-time Earthquake Damage Assessment Integrating Simulation and Sensor

By analyzing earthquake simulation results and extracting key information in advance, it becomes possible to instantly estimate the damage to all buildings in the target area once seismic data is obtained during an earthquake. In this section, we explain step by step why this approach is feasible. It is important to note how the simulation results are handled. As previously discussed, the simulations retain time-series data of building responses for each earthquake scenario. To understand an overview of the entire city's situation, visualizing these results as an overlaying map representation provides a clearer understanding. Accordingly, the system is designed to instantly generate distribution maps of risk assessment indicators. As mentioned earlier, multiple indicators can be derived from the simulation results. In this chapter, we use the representative structural response displacement obtained via CSM as an illustrative example.

3.1 Proper Orthogonal Decomposition

First, we explain Proper Orthogonal Decomposition (POD), the core technology within the proposed framework. POD is frequently used for feature extraction and dimensionality reduction in data and has been applied to numerous engineering problems in recent years. POD assumes that common modes exist across multiple sets of data. In this case, all original data can be expressed as linear combinations of these modes (multiplied by coefficients and added together). We illustrate this theory using the cat images in Figure 13 as an example.

The top row of the figure shows 10 different cat pictures. Since the color information of the pixels composing the images can be classified, this data resembles the spatial distribution of representative response displacements from simulation results in numerical values format. Using this numerical information, we extract the shared modes (patterns, distributions) present within the cat images. How this extraction is performed will be discussed later. The result yields several common modes. These are modes that exist commonly within the original data (the 10 cat images).

Among these shared modes, some are strong (highly contributory) to the original data, while others are weak. We refer to them in order of strength as the first mode, second mode, third mode, and so on. By multiplying these common modes by appropriate coefficients (POD coefficients, denoted as α in the figure) and summing them, we can fully reproduce the original data. While the coefficient values differ depending on which data is being reproduced, the common modes used remain the same. In other words, possessing information of the common modes allows the original data to be reproduced simply by varying the coefficients, enabling highly efficient data representation.

The above explanation assumes the extraction of common modes and the existence of POD coefficients, which are theoretically obtainable. We will also briefly explain this theory. First, to visually understand common modes, consider the set of two-dimensional vector data (vectors with two components) shown in Figure 14. Although the data is plotted in a two-dimensional space, it can be effectively represented by re-expressing it along the axes shown in red and blue in the figure. Specifically, by defining the first and second axes to be orthogonal to each other in order of the direction with the largest degree of data dispersion (variance), the vectors indicating those directions (u1 and u2 in the figure) are extracted as the common modes. Furthermore, since each data point can be represented as a linear combination of the modes multiplied by coefficients, controlling the strength of the modes allows all data to be represented. This process is known as the Principal Component Analysis (PCA).

Since the relationship with the aforementioned cat diagram and simulation results is difficult to grasp when the data remains as 2D vector data, a brief explanation will be added. As mentioned in the explanation of the cat diagram, while the cat diagram and simulation results can be visually classified by color for their features and patterns, they can also be considered as a numerical format. Therefore, once a rule (a rule for the direction of tracing the numbers) is established, the collection of numbers can be vectorized as shown in Figure 15. If a single figure (analysis result) consists of n numbers, the resulting vector becomes an n-dimensional vector. Furthermore, there will be n-dimensional vectors corresponding to the number of original datasets (scenarios). While the previous explanation used a 2-dimensional vector for simplicity, it is also possible to extract common modes based on the theory of principal component analysis for n-dimensional vector data, and the POD coefficient can be calculated theoretically.

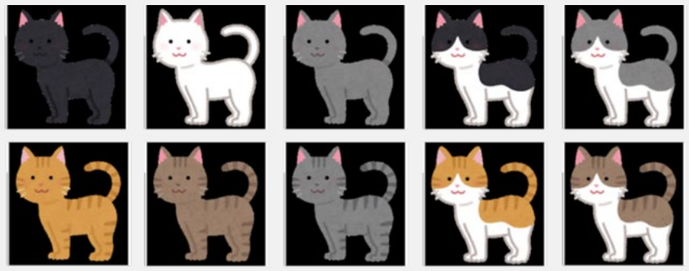

Extract Image feature

By superimposing modes, diverse cat's patterns can be expressed

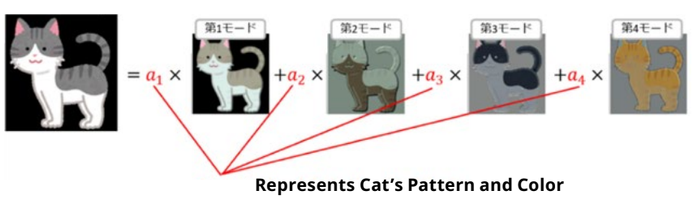

Figure 13 Illustration of POD.

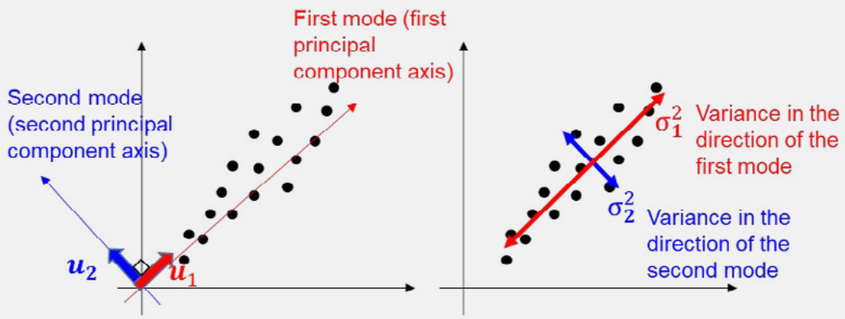

Figure 14 Illustration of PCA..

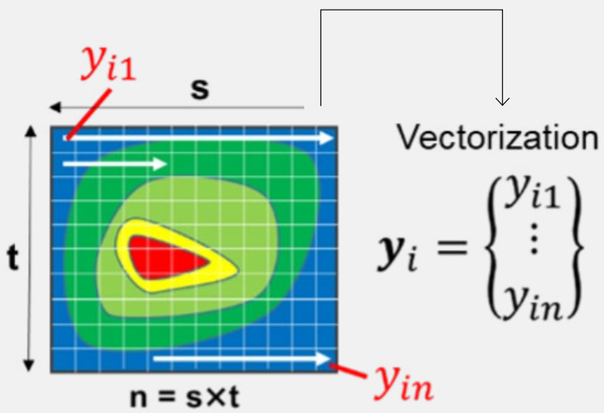

Figure 15 Illustration of vectorization.

3.2 Sparse Sensing and Optimal Sensor Placement

So far, we have explained that it is possible to calculate common modes and POD coefficients from the simulation results. Next, building on this, we will explain how simulation and sensor data are fused together.

As mentioned earlier, the original data can be represented by common modes and POD coefficients. By freely varying the POD coefficients, it is possible to generate data that does not exist in the original data. Taking the representative response displacements from the simulation results as an example, it is possible to create data that is not part of the 13 types of representative response displacements output by the simulation. Naturally, this generated data will also contain the characteristics of the common modes. Since actual earthquakes do not necessarily match the scenarios implemented in simulations, the ability to generate data beyond the original is advantageous. Furthermore, it is beneficial that this data incorporates the characteristics of common modes extracted from the simulation results. This is because, as evident from the simulation results in Figures 8 and 11, the calculated results exhibit spatial distribution tendencies specific to the target area. It is clear that common modes exist across scenarios, even when the magnitude varies between them. Furthermore, it is reasonable to assume that building damage from actual earthquakes also exhibits similar common modes. Therefore, we can hypothesize that the common modes extracted from simulation results can be applied to the building response during actual earthquakes.

If the common modes extracted from simulation results can be used to estimate building responses to actual earthquakes, then when an actual earthquake occurs, calculating the POD coefficients for each mode specific to that earthquake using some method would enable instantaneous estimation of damage to all buildings within the target area. How to determine these POD coefficients is the key to achieving the integration of simulation and sensor data. In this study, we introduced sparse sensing technology to determine the POD coefficients. Sparse sensing is a technique for estimating all the desired data through a pre-existing mathematical model when only a limited amount of measurement data can be obtained due to certain constraints. While various methods exist, the proposed framework incorporates sparse sensing technology utilizing the common modes of POD. Figure 16 illustrates this concept. In the left diagram, only some buildings are colored. Suppose seismometers are installed in these buildings, allowing us to obtain building response values when an earthquake occurs. Normally, we would only have information from the buildings with seismometers. However, using sparse sensing theory, we can estimate the responses of all buildings in the target area, as shown in the right diagram. In other words, assuming the existence of a common mode, we estimate the POD coefficients from the information of the few buildings observed. This estimation is possible by applying the theory of generalized inverse matrices in linear algebra, though detailed explanation is omitted here.

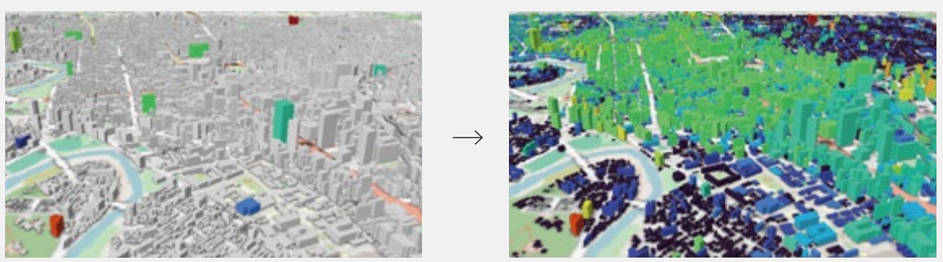

Figure 16 Concept of sparse sensing.

The theory of sparse sensing also provides information on the optimal placement of seismometers. Specifically, it indicates how to arrange seismometers within the target area to effectively estimate damage to all buildings. This involves solving an optimization problem that seeks the optimal number and placement of seismometers to accurately reproduce the original data using common-mode signals. While specific computational steps and methods are omitted here, an optimization algorithm is required, and various techniques exist for this purpose.

Figure 17 shows the result of the optimal seismometer placement calculated from the representative response displacement distribution of simulation results. The red circles indicate seismometer locations, signifying that only 13 buildings out of the total 32,334 buildings in the target area require seismometer installation. In practice, we confirmed that even 9 buildings can estimate the representative response displacement for all buildings with reasonably good accuracy.

However, results showed that accuracy gradually improved as the number of buildings with seismometers increased from 9 to 13. Therefore, the optimal configuration for 13 buildings is shown here. Note that in practice, seismometers cannot be freely installed anywhere. Therefore, it is necessary to estimate the response of other buildings using data from seismometers already installed in suboptimal locations, which will reduce estimation accuracy. However, demonstrating that such a configuration is theoretically optimal should provide valuable information for considering future disaster prevention and mitigation in the target area.

Figure 17 Optimal seismometer placement (Number of Seismometers = 13).

3.3 Verification of the Proposed Framework

This section presents the results of accuracy verification for the proposed framework's ability to estimate building damage across the entire target area. Using actual earthquake sensor data would provide the most effective verification. However, since no sensor records exist for earthquakes generated by fault movement along the Nagamachi-Rifu Fault Zone, we treated some simulation results as pseudo-real earthquake data to perform accuracy verification. Specifically, we attempted to estimate the results of scenarios with magnitudes of 6.5, 6.9, and 7.3 using information from only a small number of sensor points. Figure 18 shows the results.

The top row in the figure displays the distribution of representative response displacements obtained from the simulation results for each scenario. The second row shows the simulation results using only information from the 13 optimally placed points shown in Figure 17. In actual earthquake scenarios, similarly limited building information would be the same. The third row shows the results of estimating representative response displacement for all buildings using only the second-row information obtained from the proposed framework. If these results closely match the simulation results in the first row, this indicates good accuracy.

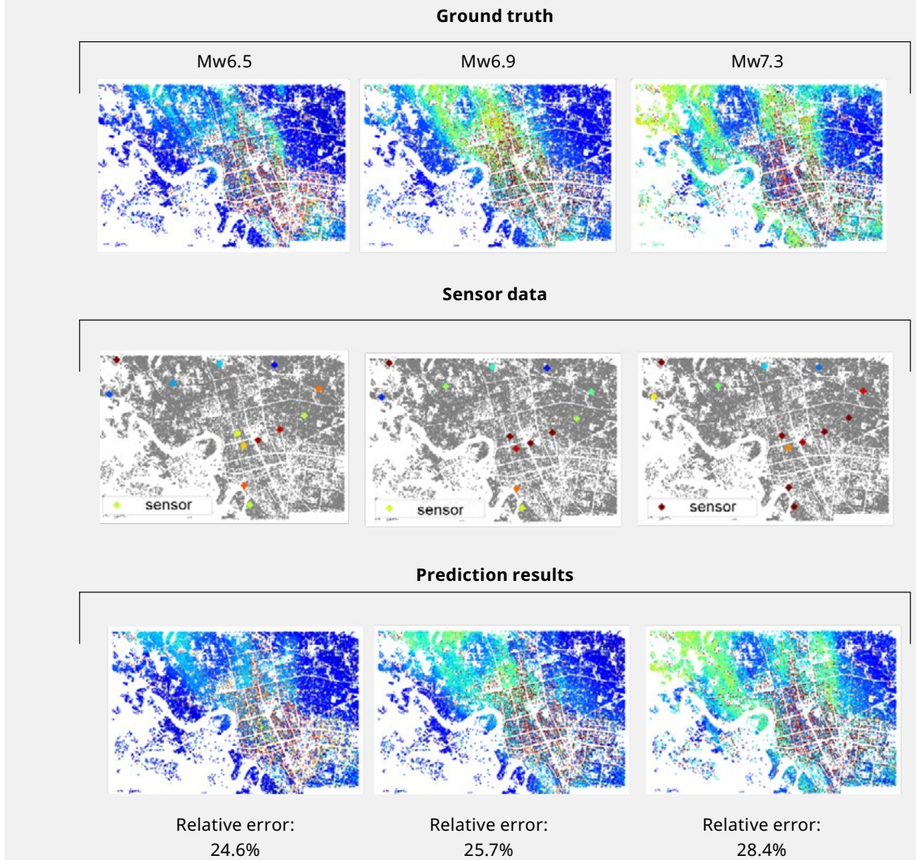

Figure 18 Verification results (accuracy verification for three scenarios).

As shown, while the estimated results partially differ from the simulation results, they capture the distribution across the entire target area with reasonably good accuracy. The average error rate for all buildings was found to be around 20–30%.

The verification results shown here are based on the condition that seismometers are theoretically optimally placed.

Therefore, we also present results under conditions where the number and placement of seismometers are not optimal. In this verification, we checked accuracy by varying the number of buildings. Figure 19 shows the results. As briefly mentioned in the optimal placement section, accuracy drops sharply with 8 or fewer sensors, while it remains reasonably good with 9 or more sensors.

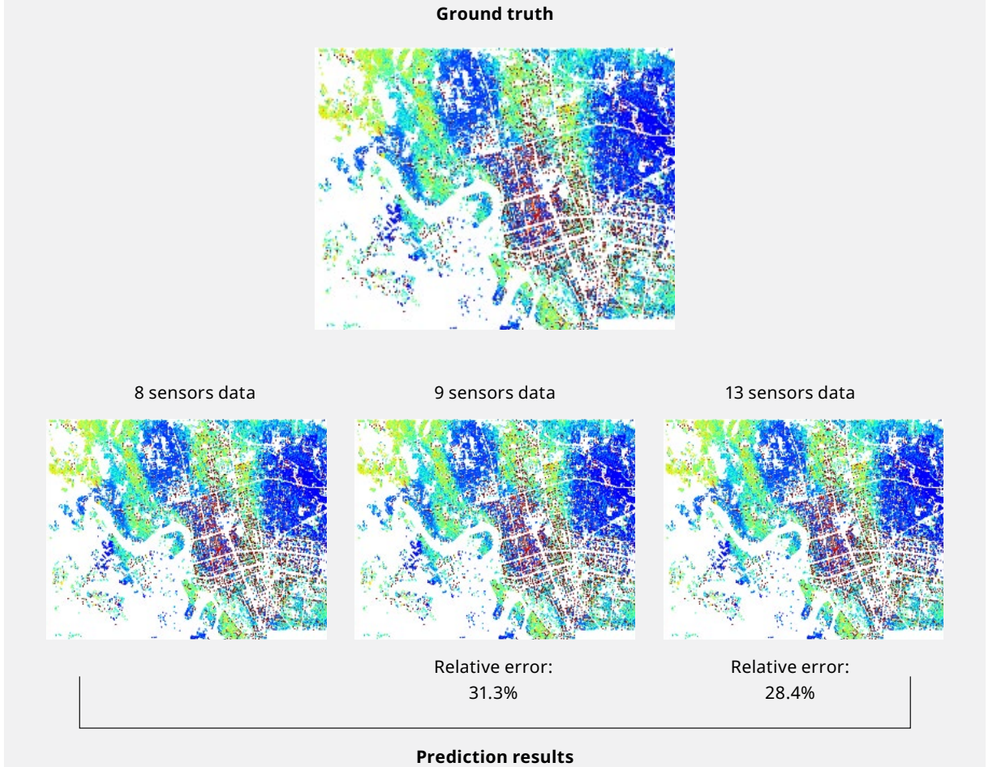

Figure 19 Verification results (accuracy comparison of different numbers of buildings with seismometers installed).

4.0
Digital Twin System “SAMRRAi”

We developed the digital twin system, Seismic Assessment and Monitoring system for Real-time Risk Analysis (SAMRRAi), as a platform for real-time earthquake damage assessment through simulation and sensor integration, contributing to enhanced urban resilience as explained in the preceding sections. Opposite, we describe its specifications and application examples.

4.1 SAMRRAi Specifications

As shown in Figure 20, SAMRRAi is a system usable both before and immediately after a disaster. Before a disaster, it can perform earthquake risk assessments for individual buildings against various predicted earthquakes by linking with simulations. It also allows the generation of seismic waveforms and the configuration of building models, ground models, and other settings for any earthquake scenario (source fault and target area). Therefore, by performing analyses for multiple earthquake scenarios, it is possible to pre-verify seismic responses to various earthquakes and create a database. Immediately after a disaster, the system can instantly provide observed values from pre-registered sensor stations (seismometers), predicted seismic response values for all buildings in the target area, and damage status assessments for structural and non-structural components.

SAMRRAi is a system that uses the open-source software QGIS as its platform, with functionality extended through QGIS plugins. QGIS is a multi-platform software that runs on operating systems such as Windows, macOS, and Linux. It not only visualizes GIS data but also provides functions for editing, analysis, and layout.

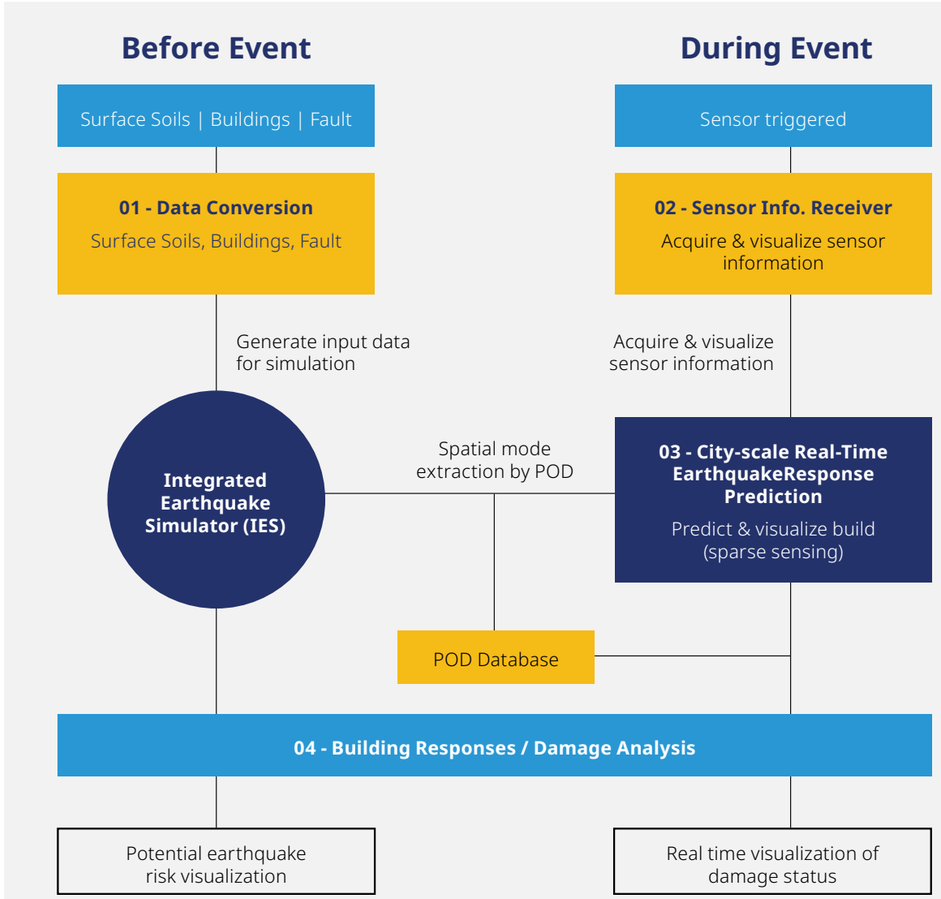

Figure 20 Evaluation workflow of the digital twin system SAMRRAi.

4.2 Application Example of SAMRRAi

Using Sendai City's Aoba Ward described in Chapters 2 and 3 as the target area, and assuming virtual sensor points (the 13 optimally placed points described in Chapter 3) exist within this area, this section presents the visualization results of a series of evaluations conducted using SAMRRAi immediately after an earthquake. Figure 21 shows the locations of assumed sensor points near Sendai Station, with red markers indicating sensor locations. It is worth noting that we can use the building response measures to determine various safety indicators (as described in Section 2.4). Furthermore, as explained in Chapter 3, by using the common modes extracted from sensor records and the results of pre-conducted simulations, it is possible to estimate the structural response values for all buildings within the target area. Here, the maximum horizontal displacement is used as an example risk assessment indicator. Figure 22 shows the results estimated for the entire target area. As can be seen in the figure, risk assessment indicators are estimated even for buildings without sensors, providing information for any building.

By using the risk assessment indicators for each building as input, the occurrence probability of different damage levels can be calculated through fragility functions. In particular, the probability of damage levels for "None" (no damage), "Slight," "Moderate," "Extensive," -concrete (RC) structures and wooden houses. For instance, Figure 23 presents a color-coded map illustrating the probability of "Complete" damage to all buildings in the study area. In addition, the numerical table in the lower right displays the evaluated probabilities together with the attributes of the building selected on the map (as indicated by the arrow in the figure). To verify the validity of these damage probability assessment results, we analyzed them by overlaying with the seismic intensity map from the 5th Earthquake Damage Estimation Survey results [7] published on Miyagi Prefecture's open data portal site. The result is shown in Figure 24. The gray areas in the figure show regions expected to experience seismic intensity 6 or higher. We confirmed that the buildings evaluated as hazardous in the damage probability distribution calculated by this system closely aligned with the gray areas on the expected seismic intensity map, validating the assessment results. Since SAMRRAi is a QGIS-based system, it allows for such overlaying with various GIS data. The ability to easily overlay its own assessment results with external GIS data is one of its key attractions.

Figure 21 Records at virtual sensor stations.

Figure 22 Risk assessment indicators for buildings other than available sensor stations (maximum horizontal displacement).

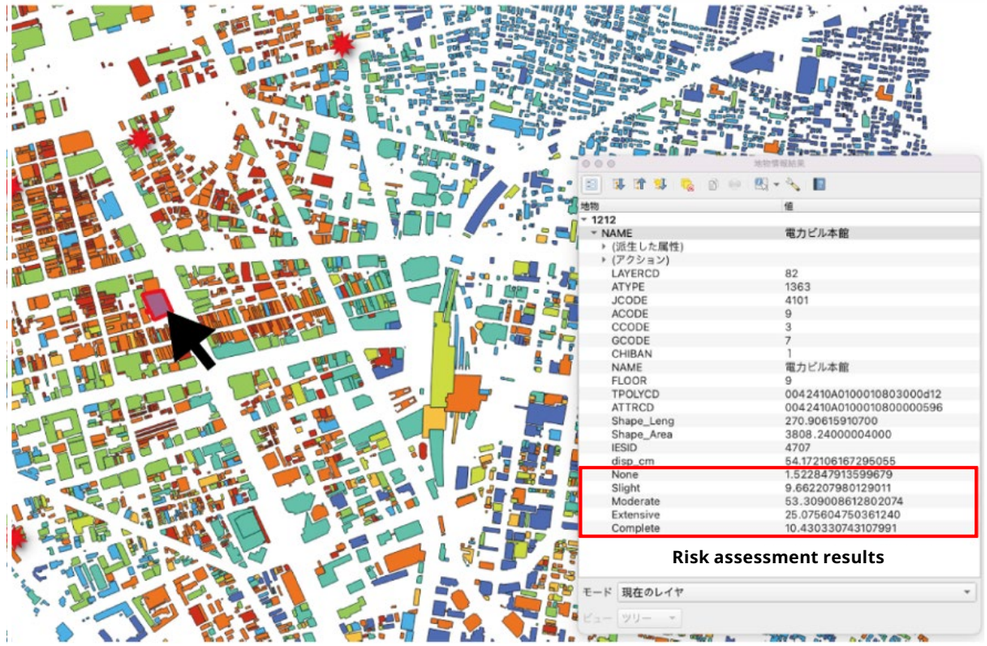

Figure 23 Probability distribution of major damage based on the fragility function.

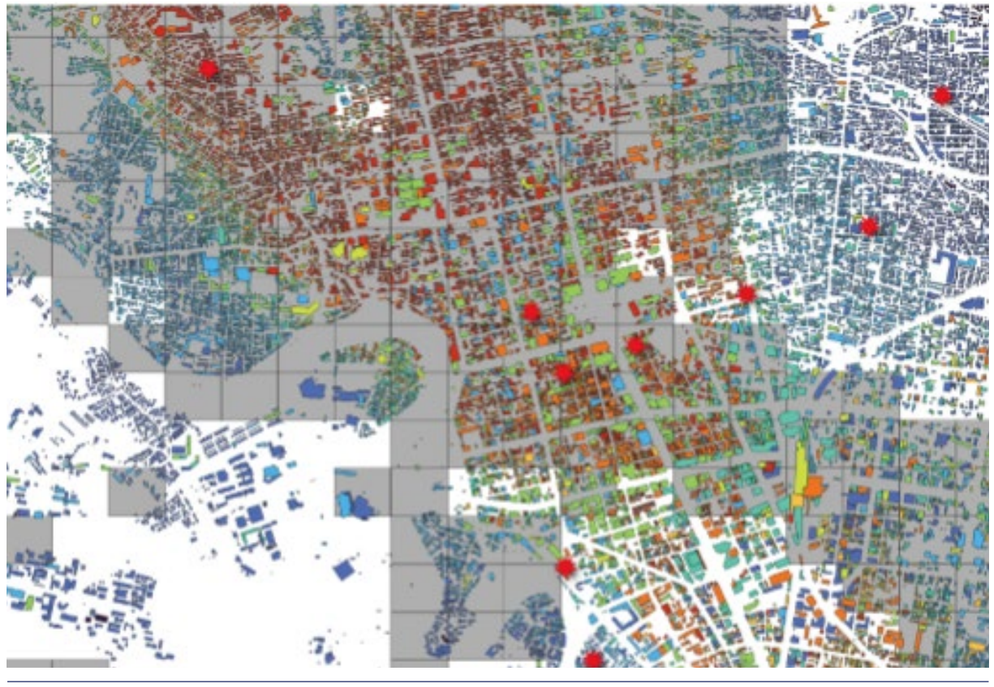

Figure 24 Comparison with the results of the fifth earthquake damage estimation Survey (gray areas indicate seismic intensity 6 or higher).

5.0 Summary

This study introduced a framework for real-time earthquake damage assessment technology that integrates simulation and sensor network to enhance urban resilience, along with SAMRRAi—a digital twin system platform implementing this technology for earthquake risk assessment. The specifications and features of SAMRRAi are summarized below.

- Generates data for earthquake risk assessment simulations and visualizes the results.
- Provides a wide range of risk assessment indicators for both structural and non-structural components, supporting both deterministic and probabilistic seismic risk assessment.
- Enables real-time risk assessment indicators for all buildings in the target area using common modes extracted from pre-run simulations and seismic sensor data.
- Integrates various GIS datasets and overlays them with its own assessment results.

Finally, we explain challenges for future implementation. The framework developed thus far enables real-time prediction of city-wide risk assessment indicators within the scope of pre-conducted simulations.

However, accurate prediction cannot be guaranteed for earthquakes not included in the simulations. For example, this study assumed an inland direct-hit earthquake from fault movement along the Nagamachi-Rifu Fault Zone. To address earthquakes from other faults, simulations targeting those specific faults must be conducted. Furthermore, when considering multiple different faults simultaneously, the common mode is likely to change depending on the considered fault, requiring enhancements to make the current framework more robust. We plan to advance research on these improvements.

Another major challenge involves input data, particularly surface ground data. For the Sendai City areas targeted in this study, existing 3D underground structure models were available, enabling us to define the target regions. However, applying this approach to other regions is not straightforward. Surface ground data is not always readily available from existing sources and creating it requires significant cost and effort. This problem is not unique to this study but is common to simulation-based, large-scale disaster risk assessments. While various datasets are being developed today, we hope that ground data databases will advance to enable easier generation of simulation input data.

References

1) J-SHIS (Japan Seismic Hazard Information Station): https://www.j-shis.bosai.go.jp/en/

2 Kamae K., Irikura K., Fukuchi Y.: Prediction of Strong Ground Motion Based on Scaling Law of Earthquake: By stochastic synthesis method, Journal of Structural and Construction Engineering, 1991, Volume 430, pp. 1-9, 1991. (In Japanese)

3) Dan K., Sato T.: Strong Motion Prediction by SemiEmpirical Method based on Variable-Slip Rupture Model of Earthquake Fault, Journal of Structural and Construction Engineering, Volume 63, Issue 509, pp. 49-60, 1998. (In Japanese)

4) J-SHIS Stochastic Green's Function Method Programs: https://www.j-shis.bosai.go.jp/map/JSHIS2/download.html?lang=en

5) Hori, M. and Ichimura, T.: Current state of integrated earthquake simulation for earthquake hazard and disaster, Journal of Seismology, Vol. 12, No. 2, pp. 307-321, 2008.

6 Federal Emergency Management Agency (FEMA): Hazus Earthquake model Technical manual, Hazus- 6.1, 2024.

7 Miyagi Prefecture: Final Report of the Fifth Earthquake Damage Estimation Surveyhttps://miyagi.dataeye.jp/resources/819. (In Japanese)

Issuer

Tohoku University International Research Institute of Disaster Science

Nippon Koei Resilient City with Digital Twin Technologies Joint Research Lab

Professor TERADA Kenjiro

Professor MORIGUCHI Shuji

SAKURABA Masaaki Visiting Professor
(Concurrent General Manager of Research & Development Center, Nippon Koei Co., Ltd.)

NOJIMA Kazuya Visiting Associate Professor
(Concurrent Specialist of Research & Development Center, Nippon Koei Co., Ltd.)

Sponsored by
Tokio Marine Holdings Inc.

Date of Issue
January 2026

TOKIO MARINE GROUP